NMR IN BIOMEDICINE, VOL. **10**, 237–249 (1997)

Implementation of Quantitative Perfusion Imaging Techniques for Functional Brain Mapping using Pulsed Arterial Spin Labeling

Eric C. Wong,[1]* Richard B. Buxton[2] and Lawrence R. Frank[2]

[1]Departments of Radiology and Psychiatry, University of California, San Diego, 9300 Campus Point Dr, La Jolla, CA 92037-7756

[2]Department of Radiology, University of California, San Diego, 410 Dickinson St, San Diego, CA 92103–8749, USA

We describe here experimental considerations in the implementation of quantitative perfusion imaging techniques for functional MRI using pulsed arterial spin labeling. Three tagging techniques: EPISTAR, PICORE, and FAIR are found to give very similar perfusion results despite large differences in static tissue contrast. Two major sources of systematic error in the perfusion measurement are identified: the transit delay from the tagging region to the imaging slice; and the inclusion of intravascular tagged signal. A modified technique called QUIPSS II is described that decreases sensitivity to these effects by explicitly controlling the time width of the tag bolus and imaging after the bolus is entirely deposited into the slice. With appropriate saturation pulses the pulse sequence can be arranged so as to allow for simultaneous collection of perfusion and BOLD data that can be cleanly separated. Such perfusion and BOLD signals reveal differences in spatial location and dynamics that may be useful both for functional brain mapping and for study of the BOLD contrast mechanism. The implementation of multislice perfusion imaging introduces additional complications, primarily in the elimination of signal from static tissue. In pulsed ASL, this appears to be related to the slice profile of the inversion tag pulse in the presence of relaxation, rather than magnetization transfer effects as in continuous arterial spin labeling, and can be alleviated with careful adjustment of inversion pulse parameters. © 1997 John Wiley & Sons, Ltd.

NMR in Biomed. **10**, 237–249 (1997) No. of Figures: 12 No. of Tables: 0 No. of References: 18

Keywords: perfusion; arterial spin labeling; BOLD; QUIPSS

Received 25 February 1997; revised 20 May 1997; accepted 21 May 1997

INTRODUCTION

In functional magnetic resonance imaging (fMRI) of the brain, blood oxygenation level dependent (BOLD) techniques[1] are typically used because they provide a high functional contrast to noise ratio. The analysis and interpretation of BOLD contrast functional data is complicated by the fact that the MRI signal change is related to the underlying neuronal activation through local blood flow, blood oxygenation, and blood volume changes. Arterial spin labeling (ASL) techniques are capable of providing quantitative information about local tissue blood flow, by observing the inflow of magnetically tagged arterial blood into an imaging slice. The term flow is used here to be synonymous with perfusion (volume of blood delivered to capillary beds per unit volume of brain tissue per unit time). For fMRI, these techniques are of interest for three major reasons: they measure a quantity (cerebral blood flow (CBF)) that is thought to be more directly related to neuronal activation than the BOLD signal;[2] the flow signal may be spatially more well localized to the site of neuronal activity; and they can measure baseline CBF in addition to changes in CBF. ASL is useful both as a measurement technique for functional neuroimaging applications, and as a tool for the study of functional neuroimaging techniques such as BOLD contrast imaging.

We detail here our implementation of several forms of pulsed ASL and discuss and demonstrate experimental conditions in its application to fMRI. The analysis here is divided into four broad categories: tagging methods; perfusion quantitation; simultaneous perfusion and BOLD data acquisition; and multislice perfusion imaging. The methods and results section are each subdivided into these categories.

METHODS

The prototype pulse sequence that we use for functional ASL is shown in Fig. 1. The first saturation pulse is slice selective and applied in the imaging slice. Immediately following this in-plane saturation, the inversion tag is applied. In most cases, a second saturation pulse is applied after a delay TI_1 and after an additional delay, an image is acquired using single shot EPI at time TI_2 after the inversion tag. The details and rationale for this pulse sequence design are described here.

Correspondence to: Eric C. Wong; *e-mail:* ecwong@ucsd.edu

Abbreviations used: ASL, arterial spin labeling; BOLD, blood oxygenation level dependent; CBF, cerebral blood flow; EPISTAR, echo-planar imaging with signal targetting using alternating RF; FAIR, flow alternated inversion recovery; fMRI, functional magnetic resonance imaging; MRI, magnetic resonance imaging; MT, magnetization transfer; PICORE, proximal inversion with a control for off resonance effects; QUIIPSS II, quantitative imaging of perfusion using a single subtraction (version II); RF, radiofrequency; SNR, signal-to-noise ratio.

 CCC 0952–3480/97/040237–13 $17.50

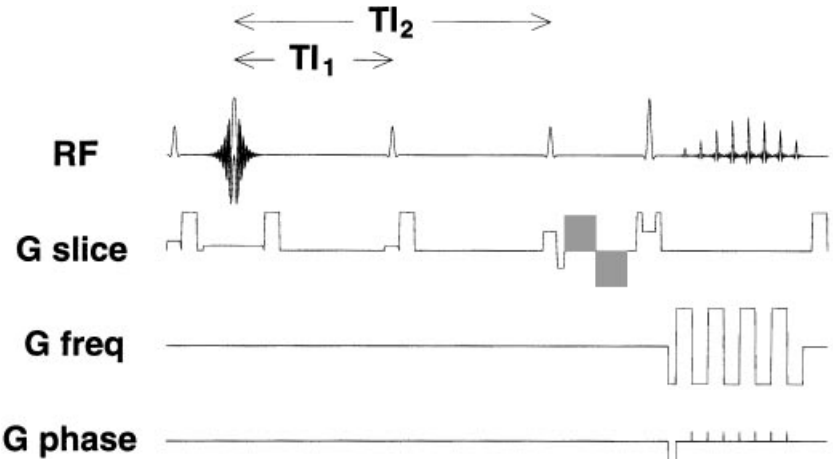

Figure 1. Pulse sequence for pulsed arterial spin labeling. RF pulses from left to right are: (1) in-plane presaturation; (2) inversion tag; (3) QUIPSS II saturation (see text); (4) 90° excitation pulse; (5) 180° refocussing pulse (optional for spin echo). Not shown is a narrow bandwidth fat saturation pulse and crusher gradient immediately prior to the excitation. The bipolar gradients shown shaded are flow weighting gradients for dephasing of flowing spins (optional).

Arterial tagging methods

We use three different methods for applying the pulsed arterial tag: EPISTAR;[3] a derivative of EPISTAR that we refer to as PICORE (proximal inversion with a control for off-resonance effects); and FAIR.[4] These techniques differ in their sensitivity to inflow from the distal side of the slice and in their tag profiles. In all cases, imaging is alternated between two states, one in which blood proximal to the imaging slice is inverted at time *TI* prior to imaging (referred to as the tag state), and one in which inflowing blood is not inverted (referred to as the control state). The fundamental signal in these experiments is the difference signal between these states (control–tag). The tagging profiles for these three techniques are depicted graphically in Fig. 2. In EPISTAR the tag is applied using a slab selective inversion proximal to the imaging slice, while the control is a slab selective inversion distal to the imaging slice. In PICORE the tag is identical to that of EPISTAR, but the control is an off resonance inversion pulse that is applied at the same frequency offset relative to the imaging slice as the tag, but in the absence of a slab selective gradient. In FAIR the tag is applied using a non-selective inversion pulse, and the control is a slice selective inversion applied to the imaging slice. In the subtraction images (control–tag), blood that flows into the imaging slice from the proximal side will register as a positive signal for all three techniques, while tagged blood flowing into the distal side will register as positive signal in FAIR, as negative signal in EPISTAR, and as no signal in PICORE.

The choice of one of these tagging techniques should depend in part on what is known about the geometry of the blood supply to the slice/area of interest. If arterial blood is entering the slice from a known direction, then PICORE tagging is natural because it only tags blood from one side. However, in watershed areas or other areas where the geometry of the arteries does not consistently enter through a known side of the slice, such as a parasagittal slice, FAIR is a conservative technique to assure that inflowing arterial blood does not evade the tag. From a tagging point of view, EPISTAR would not be preferable over PICORE or FAIR. However, if gradient eddy currents from the slab selective inversion pulse are significant, then EPISTAR may be preferred because it uses identical slab select gradients for the tag and control states, while both PICORE and FAIR use a slab select gradient for one state but not the other, possibly leading to systematic errors in the subtraction.

An additional consideration in the choice of tagging technique is the slice profile of the inversion pulse. For a given RF inversion pulse, the ratio of the width of the pulse to the width of the transition is fixed, so that a narrower

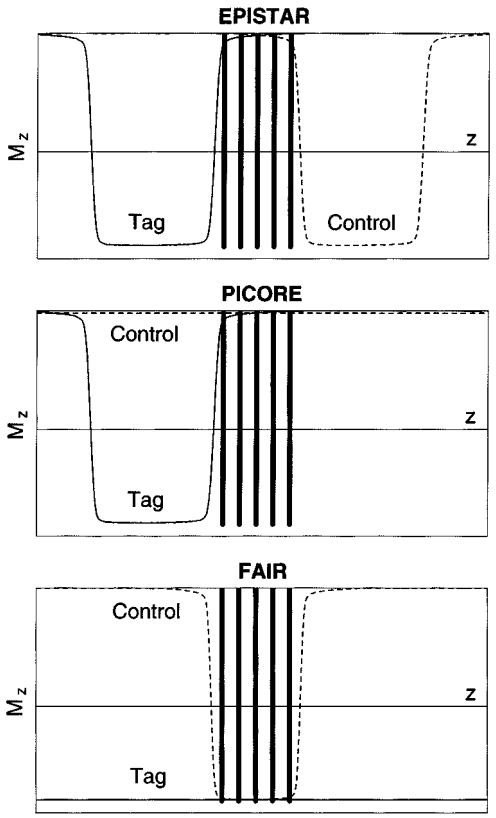

Figure 2. Inversion profiles of tag and control pulses for EPISTAR, PICORE and FAIR. The tag profile is solid, and the control profile is dashed. Example slice locations for a five slice experiment are shown as bold vertical lines. At each slice location, the static tissue contribution to the difference signal is the difference between the tag and control profiles. The inversion profile shown was measured experimentally in an aqueous phantom using a 30 ms hyperbolic secant pulse with parameters $\mu = 10$ and $\beta = 400\ s^{-1}$.

inversion gives a sharper slice profile. For FAIR, which typically uses a thinner inversion slice profile than EPISTAR or PICORE, the profile of the edge of the tag is sharper, which is helpful in the quantitation of CBF. For single slice imaging the inversion in FAIR is almost always narrower than in EPISTAR or PICORE, but this may not be true for multislice measurements where the FAIR control inversion must encompass all slices. Another related difference is that the tag region for FAIR is defined on the distal end (toward the imaging slice) by the RF pulse, but on the proximal end by the B_1 profile of the RF coil. For EPISTAR and PICORE, the tag region is entirely defined by the RF pulse (provided the defined inversion slab lies within the sensitivity range of the RF coil).

Perfusion quantitation

There are two related vascular effects that create systematic errors in the quantitation of CBF.[5] One is the transit delay between the application of the tag and the arrival of tagged blood into brain tissue in the imaging slice. The second is the inclusion of intravascular signal from tagged blood that is destined to perfuse more distal slices as perfusion of the imaging slice. Both are related to the fundamental problem that the time required for tagged arterial blood to travel from the tagging region to the capillary is similar to the T_1 of blood. This makes it necessary to acquire the image while many dynamic processes are taking place (delivery, exchange, clearance by T_1 and flow). If images are acquired too early after application of the tag, then CBF can be underestimated because of the presence of the transit delay, or overestimated because of tagged intravascular signal traveling through the imaging slice. If images are acquired a long time after the application of the tag, then the tag signal is small due to T_1 decay, and more difficult to quantify because the tagged blood water exchanges into brain tissue where the rate of T_1 decay is different from that of blood. Approaches to minimizing these sources of error are described below.

We use a simple kinetic model[6] to describe the inflow of tagged blood into the imaging slice. At time $t=0$, an inversion tag is applied proximal to the imaging slice. After a transit delay δt, tagged blood begins to flow into the slice. This delay δt varies across a slice and also varies with activation. For a tag with a time width of τ (physical tag width/average velocity along the tag axis through the tagging region), the amount of tagged magnetization that has entered the slice increases linearly during the time period $\delta t > t > \delta t + \tau$, and clears due to T_1 decay and outflow. The difference signal (control–tag) is given by

$$\Delta M(t) = \begin{cases} 0 & t < \delta t \\ 2M_{0B} f (t - \delta t) e^{-t/T_{1B}} q(T_{1B}, T_{1T}, T_{ex}, f, \lambda, t) & \delta t < t < \delta t + \tau \\ 2M_{0B} f \tau e^{-t/T_{1B}} q(T_{1B}, T_{1T}, T_{ex}, f, \lambda, t) & \delta t + \tau < t \end{cases} \quad (1)$$

where M_{0B} is the relaxed magnetization of arterial blood, f is the CBF in mL-blood/mL-tissue/min, T_{1B} is the T_1 of arterial blood, and T_{1T} is the T_1 of brain parenchyma. T_{ex} is the transit time from the distal edge of the tag region to the capillary bed where tagged blood water exchanges into brain parenchyma. q is a correction factor for the fact that the rate of decay of the tag switches from that of blood to that of tissue after exchanging into tissue, and for clearance of the tag by flow. Under most conditions, q is close to unity. The shift of the decay rate of the tag from that of blood to that of tissue occurs after the tagged blood not only reaches the slice but exchanges into tissue. From diffusion weighted data[7] this exchange appears to occur typically 1000 ms or more after the application of the tag. The second contribution to q is the clearance of the tag by flow. Because there is nearly complete exchange of arterial water with tissue water in the capillary bed, the clearance of tagged water by flow is much slower than the delivery of tagged water. Assuming complete exchange of water between blood and brain tissue, the rate constant for clearance of tagged water is simply equal to flow. A typical value for CBF is 60 mL/100 mL/min, giving a rate constant of 0.01 s^{-1}. The rate constant for the clearance of tagged water by T_1 decay is $1/T_1$, or about 1.1 s^{-1}. Thus the clearance of the tag is dominated by T_1 decay, and clearance by flow is likely to be insignificant. In practice it is difficult to determine q exactly because it depends on the details of the exchange of water between blood and tissue, which is not well understood. Fortunately, the value of q is both near unity and not very sensitive to variations within reasonable ranges of the parameters it depends on. If we assume that blood water exchanges instantly and completely with tissue water upon reaching the capillary bed, and that tissue water follows single compartment kinetics, then q is given by

$$q(t) = \int_0^{(t-T_{ex})} e^{-t'/T_{1B} - (t - T_{ex} - t'))/T'_{1T}} dt' \Big/ (t - T_{ex})\, e^{-(t-T_{ex})/T_{1B}} \quad (2)$$

for $t > T_{ex}$ and $t > \delta t + \tau$, where

$$\frac{1}{T'_{1T}} = \frac{1}{T_{1T}} + \frac{f}{\lambda}, \quad (3)$$

and λ is the brain-blood partition coefficient of water. The denominator of eq. (2) is the T_1 decay of the tag in the time period $t > T_{ex}$ if $T_{1T} = T_{1B}$, and the numerator is the T_1 decay in the same time period in the presence of exchange into tissue with decay constant T_{1T}. As an example, if $t = 1400$ ms, $T_{ex} = 1000$ ms, $T_{1B} = 1300$ ms, $T_{1T} = 900$ ms, $f = 0.01$ s^{-1} and $\lambda = 0.9$, then $q = 0.93$.

It is important to note that the expressions given here for the difference signal assume that the parameters δt, τ, T_{ex}, etc., are uniform across each voxel, which is certainly not true. The actual signal is an average across heterogeneous populations of vessels and tissues, but we start with these simple expressions to determine how well they can describe experimental data and provide insight into the contrast mechanisms.

Transit delay

It is clear from eq. (1) that for a given flow f, the measured signal can be very much dependent upon the value of the transit delay δt. We have determined experimentally that this delay ranges from about 500–1500 ms for a physical gap of 1–3 cm between the tag region and the imaging slice. Because the inversion time TI used for the imaging cannot be much larger than this range due to T_1 decay of the tag, this delay is potentially a very significant source of

systematic error in the flow measurement. One approach to this problem is to collect data at two or more different values of TI and estimate both δt and f.[5] While this is effective, it is not time efficient, and reduces the SNR of the measurement by requiring an additional signal subtraction. We currently use a technique that we refer to as QUIPSS II (quantitative imaging of perfusion using a single subtraction — second version)[8] in order to obtain quantitative perfusion data that is insensitive to variations in δt. An earlier version (QUIPSS) is described in,[9] but is more susceptible to artifacts from intravascular signal. In QUIPSS II, at time TI_1 after the application of the tag, a saturation pulse is applied to the tagging region in both tag and control states, thus effectively cutting off the tail end of the inflowing tag. This delivers a bolus of tagged blood of time width TI_1 to the imaging slice. After an additional delay, an image is acquired at time TI_2. If

$$TI_1 \leqslant t \tag{4}$$

and

$$TI_2 \geqslant TI_1 + \delta t \tag{5}$$

then the signal is independent of both δt and τ, and is given by

$$\Delta M = 2M_{0B} f TI_1 \, e^{-TI_2/T_{1B}} q(T_{1B}, T_{1T}, T_{ex}, f, \lambda, t). \tag{6}$$

The condition on TI_1 is that it is shorter than the natural time width of the tagged bolus. If this is satisfied then the time width of the bolus is known to be TI_1. The condition on TI_2 is required to allow for the delivery of the entire bolus to the imaging slice. If this is satisfied, then the flow f can be calculated directly from eq (6). If M_{OB} and T_{1B} (both global constants) are known, then f can be quantified in absolute units. If these constants are not known, then quantitative maps of relative perfusion can still be made from ΔM alone, and these maps are consistent in scale both across the image and through time in a functional time series. For functional perfusion imaging, we typically neglect q, as it is both near unity and relatively insensitive to changes in flow. Note that eq. (6) holds even if the bolus of tagged blood is not delivered by plug flow as is implied by eq. (4). If there is dispersion of the tag due to a distribution of flow velocities, then if eq. (5) holds for the longest δt, then the entire tagged bolus will still be delivered to the imaging slice and eq. (6) is valid.

Intravascular signal

A second source of systematic error that is related to the dynamics of the circulation is the inclusion of tagged intravascular signal in the perfusion measurement from vessels that are passing through, but not perfusing, the imaging slice. Signal from these vessels are not properly interpreted as perfusion of the imaging slice because they will end in capillary beds in more distal slices. One approach that has been used for minimizing this source of artifact is the application of additional bipolar gradient pulses to dephase the magnetization of flowing spins in larger vessels. Such gradients will be referred to here as flow dephasing gradients. This has been shown to significantly increase the measured transit delay,[10] indicating that much of the tagged signal that appears at early TI is intravascular. However, it is difficult to determine what portion of this intravascular signal is destined for the imaging slice and what portion is flowing through to more distal slices. A second approach is to simply image at relatively long TI, so as to allow blood that is flowing through the imaging slice to do so before the image is acquired. A convenient feature of QUIPSS II is that imaging at long TI_2 has little effect on the quantitation of perfusion, except of course for increased T_1 decay of the tag. In practice, we use values of TI_1 in the range of 600–700 ms, and TI_2 in the range 1200–1400 ms, which is typically the time at which focal signals from arteries disappear from the difference signal, and also the earliest values of TI_2 at which small amounts of flow weighting have minimal effect on the perfusion signal. QUIPSS II is used both because it can be made insensitive to the transit delay δt, and because it creates a well defined trailing edge of the bolus of tagged blood which allows for clearance of intravascular tag before acquisition of the image. This technique for avoiding vascular artifacts is in principle very similar to recently introduced versions of the continuous ASL technique, where the inversion is stopped and a delay inserted before imaging acquisition.[11]

Simultaneous perfusion and BOLD imaging

A powerful feature of ASL techniques for fMRI is that they can be used to simultaneously acquire quantitative perfusion data and BOLD contrast data. If a gradient echo, asymmetrical spin echo, or long TE spin echo is used for image acquisition, then BOLD contrast is present in the image series. In order to separate the perfusion signal from the BOLD signal, it is critical that the in-plane presaturation be applied (see Fig. 1). Because of this presaturation, the longitudinal magnetization M_z of the inflowing blood in the tag state is smaller by exactly M_{OB} than the M_z of the blood/tissue it is replacing immediately after inversion. Similarly, the M_z of the inflowing blood in the control state is larger after the control pulse than that of the blood/tissue it is replacing by exactly the same amount (M_{OB}). Thus the tag condition is negatively flow weighted (inflow decreases M_z), while the control condition is positively flow weighted (inflow increases M_z). The difference signal between control and tag states is directly proportional to $2M_{OB}$ (eq. (1)), while the average of control and tag signals is approximately independent of flow, and can be used as a BOLD time series. In fact, if the T_1 of the tissue is identical to that of blood, then the average of the tag and control states is precisely independent of flow. The sum of the magnetization of the inflowing blood in the tag and control states follows a saturation recovery curve (inversion recovery in the tag state + relaxed magnetization in the control state). Because of the in-plane presaturation, the static tissue is also following a saturation recovery curve, and inflow does not affect the net M_z in the imaging slice.

However, because the T_1 of blood is known to be longer than that of tissue, there is some residual negative flow weighting in the average due to exchange of blood water with tissue water. This residual flow contribution can be estimated by calculating the difference between the magnetization of the tissue compartment in the presence and in the absence of inflow for a saturation recovery experiment. For a QUIPSS II experiment with $TI_1 = 700$ ms, $TI_2 = 1400$ ms, $\delta t = 1000$ ms, $T_{1B} = 1300$ ms, and $T_{1T} = 900$ ms, the residual flow signal in the average of tag and control images is approximately 18% of the flow signal in the difference signal between tag and control states. This flow contribution has the opposite sign as that of the BOLD signal, and thus

can only cause underestimation of the BOLD signal.

BOLD effects can also contaminate perfusion measurements, but this effect is probably even smaller than the effect of flow on the BOLD signal. To a first approximation, the BOLD effect causes a simple scaling of the MR signal on the order of 2–4% during activation. If this scaling occurs uniformly throughout the tissue, then this would result in a simple scaling of the flow difference signal. A typical value for the SNR of the flow measurements is approximately 20 for 3 min of averaging, so changes on the order of 2–4% would be at the limit of detectability. Furthermore, functional changes in the flow signal are typically on the order of 50% of the flow signal, and would dominate BOLD related changes. However, the distributions of tissue that give rise to the flow and BOLD signals are different, and may result in a more complex interaction between the flow and BOLD signals. The flow signal arises mostly from small arteries, capillaries, and brain parenchyma. This is demonstrated in the fact that the early *TI* flow signal is greatly attenuated by small flow weighing gradients, and distributes into tissue at longer *TI*. The BOLD signal is primarily from veins and tissue surrounding veins, and cannot arise from the arterial side of the circulation because arterial oxygenation is essentially constant. The only overlap between the populations of tissues that give rise to flow and BOLD signals is in brain parenchyma surrounding veins. These extravascular tissues are responsible for only about one third of the BOLD signal as determined by diffusion weighted BOLD studies,[12] and thus produce signal changes that are on the order of 1%, generating errors in the flow measurement that are typically within the experimental error.

Multislice ASL

A practical issue that is critical to the utility of flow imaging is the extension of the technique to multislice imaging. Unfortunately, this extension is not straightforward. Because ASL involves tagging a large area of tissue proximal to the imaging slice, multislice imaging cannot be performed in an interleaved manner as in conventional imaging, and sequential imaging of multiple slices would be prohibitively slow. A natural way of implementing multislice ASL is to apply an inversion tag, and then after a delay rapidly acquire images from multiple slice locations distal to the tag. Two complications that are more prevalent in this scheme than in single slice ASL are increased transit delays to the more distal slices, and poor subtraction of static tissue between tag and control states.

In a multislice application, the transit delay between the tagging region and the more distal slices can be long (greater than 1 s). We have determined experimentally that the mean transit delay increases by approximately 150 ms for each additional 1 cm gap between the tagging region and the imaging slice. Because the transit delay is both longer and more variable across a slice than in single slice imaging, it is important to use a technique such as QUIPSS II that is relatively insensitive to variations in the delay. In our implementation, we apply an inversion tag followed by the QUIPSS II saturation pulse, and after a delay collect multislice images in rapid succession sequentially from proximal to distal. This sequence for image acquisition in principle allows for the possibility that acquisition of a proximal imaging slice destroys tagged magnetization that is destined for a more distal slice, thus creating an artifactual reduction of the measured flow in the more distal slice. However, in order for this to happen, tagged blood would have to be flowing faster than the progression of image acquisition across the slices. We typically collect images at a rate of one per 80 ms, with slice locations separated by 6 mm, giving a velocity of 7.5 cm/s. Based on the measured dependence of transit delay upon the separation between the tag and the imaging slice, we estimate an average velocity of tagged blood near the destination slice of approximately 6 cm/s, indicating that the faster flowing vessels could suffer from this artifact. However, this would require that the faster flowing tagged blood is also the latest to arrive in the slice, which is not likely. For QUIPSS II multislice experiments, it is important the TI_2 for the more distal slices is long enough to satisfy eq. (4), and to allow for outflow of tagged blood that is flowing through the slice. For a five slice experiment, we typically collect the first slice at $TI_2 = 1200$ ms and the last at $TI_2 = 1520$ ms. This value for TI_2 for the last slice may not be long enough to allow for delivery of the entire tag and flow through of intravascular tag, but is a compromise between these effects and diminishing SNR due to T_1 decay. For studies in which quantification of flow is paramount, longer *TI* (and more averaging to improve SNR) may be advisable.

The second complication that accompanies multislice ASL is the consistency of the static tissue signal between tag and control states. Because the perfusion signal is small ($\approx 1\%$), it is critical that the subtraction of static tissue signal between tag and control states be accurate. In both continuous and pulsed ASL, only one slice location receives exactly the same RF radiation in tag and control states. Imperfect static tissue subtraction away from this location has been attributed to magnetization transfer (MT) effects for continuous ASL.[13] We have found that in pulsed ASL, the observed imperfections in the static tissue subtraction are entirely consistent with simple slice profile effects of the tag and control pulses. The source of this effect is demonstrated schematically in Fig. 2 for the three tagging schemes. In each panel, the solid and dashed lines represent the distribution of longitudinal magnetization created by the tag and control RF pulses, respectively. The quality of static tissue subtraction is given by the distance between the solid and dashed lines at each slice location (vertical bars). The relevant portions of the slice profile for EPISTAR and PICORE are just outside of the inversion band, while the flatness of the inversion band itself is critical for FAIR. In all cases, the subtractions are dramatically improved by applying a presaturation pulse to the imaging slices immediately prior to the inversion tag, because this nominally destroys all magnetization in the slices and minimizes the in-slice effects of the tag pulses, but residual errors are often significant. Even for single slice imaging, the control and tag profiles are only identical at the center of the slice, and through slice variations are often detectable as imperfect subtractions. The inversion profile shown in Fig. 2 was experimentally measured in a simple aqueous phantom that does not demonstrate MT effects, using a hyperbolic secant (sech) pulse[14] with parameters $\mu = 10$ and $\beta = 400\ s^{-1}$, truncated at 30 ms width. These sech parameters were initially chosen because at the B_1 amplitude used (0.147G) this sech pulse exceeds the adiabatic condition by approximately a factor of 2 (determined empirically), and allows for efficient inversion in the presence of B_1 inhomogeneity in the RF coil. This B_1 amplitude is used because it is the amplitude of a 3.2 ms 180° single sidelobe

sinc pulse, which is the reference B_1 within the pulse sequence code. However, it was later determined that the quality of the inversion slice profile is critically dependent upon the parameter β, and that the profile is optimized with the highest value of β that minimally satisfies the adiabatic condition at the available B_1 amplitude.

In order to better understand these effects, we examined both theoretically and experimentally the slice profile of sech pulses in the presence of T_1 and T_2 relaxation.[15] Using direct simulation of the Bloch equations with relaxation, the slice profile of a sech pulse with the above parameters was calculated and is shown in Fig. 3(a) for a sample with infinite T_1 and T_2 and a sample with $T_1 = 900$ ms and $T_2 = 80$ ms. Note that at finite T_1 and T_2, the simulated profile is degraded near the transition region both inside and outside of the inversion band, and is slightly asymmetrical. The quality of the profile near the transition is dominated by T_2 decay that occurs while the magnetization is adiabatically brought away from the *Z*-axis, while the asymmetry of the profile is dominated by T_1 decay of the spins that are inverted earlier in the pulse. In an aqueous solution of NaCl and $CuSO_4$ that does not exhibit MT effects but has similar relaxation parameters as in the simulation, the slice profile of this same pulse was measured using a conventional FLASH sequence with the sech pulse applied in the readout direction as a prepulse. The experimental profile is also shown in Fig. 3(a) and is in very good agreement with the simulated profile. The deviations from an ideal slice profile are large enough to account for the imperfections that are seen in multislice pulsed ASL experiments. By simply increasing β to 800 s^{-1} and shortening the pulse by a factor of two, the theoretical and measured slice profiles are greatly improved, and are shown in Fig. 3(b). This sech pulse was used in the experiments described below.

Scan parameters

Imaging was performed on a clinical 1.5 T GE SIGNA system with inserted local head gradient and RF coils of our own design. The gradient coil is a three-axis symmetrical design that generates greater than 20 mT/m on all three axes at 100 A with rise times of <100 μs.[16] The RF coil is an elliptical endcapped quadrature transmit-receive birdcage coil.[17] Subjects were healthy volunteers, ranging in age from 19 to 42. All imaging was performed using single shot blipped EPI, either gradient recalled or spin echo, at 64×64 matrix size with a data acquisition time of 40 ms. Fat saturation was applied using a 16 ms 90° single sidelobe sinc pulse followed by a crusher gradient prior to imaging. FOV was typically 24 cm × 8 mm, for an in-plane resolution of 3.75 mm.

In a typical combined flow and BOLD functional study, we use PICORE/QUIPSS II, and gradient recalled EPI with a *TE* of 30 ms. For flow without BOLD, we use spin echo EPI at a *TE* of 45 ms to achieve better image quality and insensitivity to susceptibility related signal dropouts. For flow imaging with flow weighting gradients, we apply a bipolar gradient pulse of amplitude 0.65 G/cm and total duration 16 ms between the 90° and 180° pulses of a spin echo EPI sequence. Typical scan parameters are *TR* 2 s, $TI_1 = 600$–700 ms, $TI_2 = 1200$–1400 ms, a 10 cm tag with a 1 cm gap between the tag and the imaging slice. In-plane presaturation is applied using a slice selective pulse that is twice the thickness of the imaging slice. The QUIPSS II saturation pulse is a sinc pulse with eight zero crossings on each side of center. For functional studies, volunteers were instructed to perform rapid self paced bilateral sequential finger tapping alternating with periods of rest.

The choice of *TR* in pulsed ASL experiments is unusual

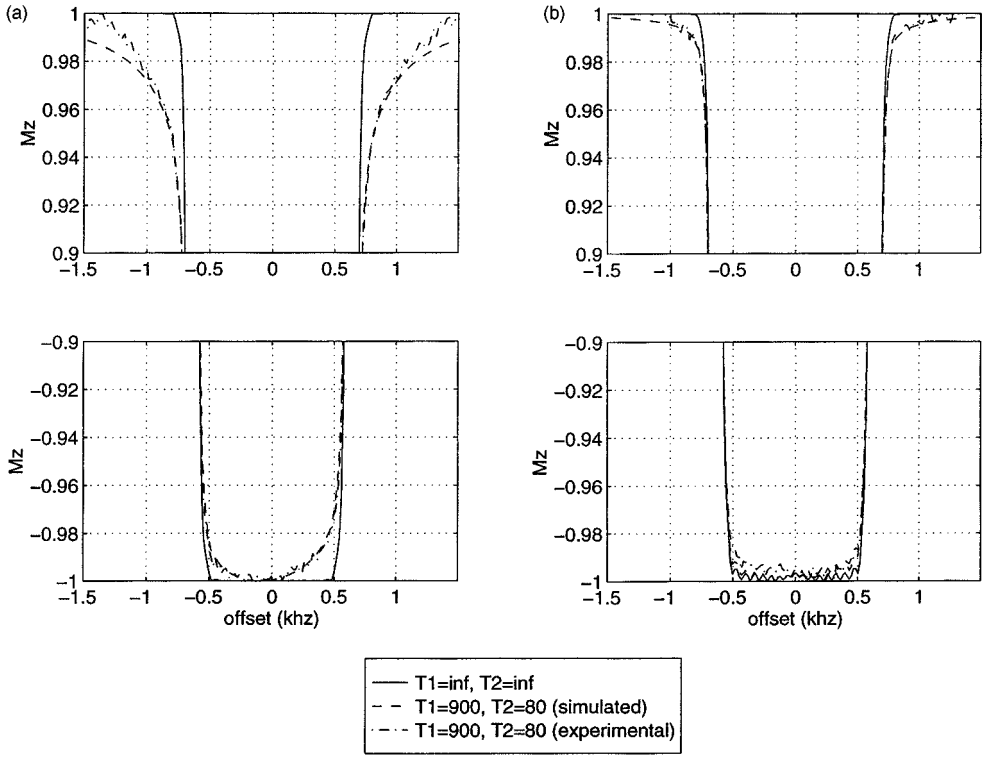

Figure 3. Calculated and measured inversion profiles for sech pulses. Note broken scale to enlarge differences between profiles. In each panel profiles are: calculated for $T_1 = T_2 = \infty$; calculated for $T_1 = 900$ ms and $T_2 = 80$ ms; and measured experimentally in a phantom with $T_1 \approx 900$ ms and $T_2 \approx 80$ ms. (a) $\mu = 10$, $\beta = 400$ s^{-1}, truncated at 30 ms. (b) $\mu = 10$, $\beta = 800$ s^{-1}, truncated at 15 ms.

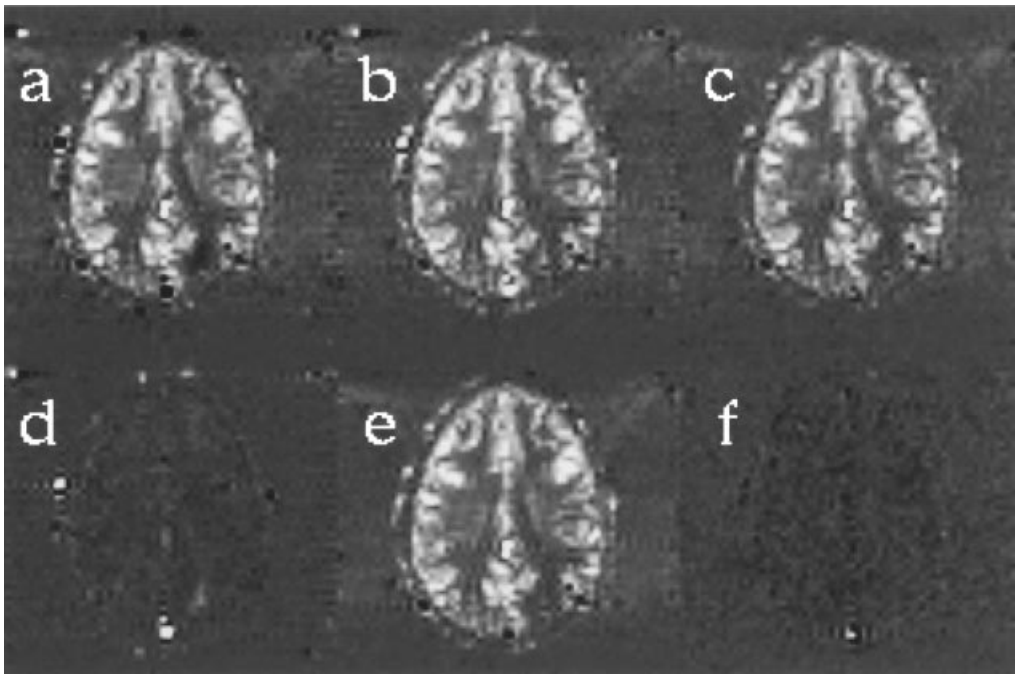

Figure 4. EPISTAR, FAIR and PICORE difference images at *TI*=1100 ms. (a) EPISTAR. (b) FAIR. (c) PICORE. (d) FAIR-EPISTAR (b–a). (e) (FAIR+EPISTAR)/2. (f) PICORE-(FAIR+EPISTAR)/2. Differences between EPISTAR, FAIR and PICORE are dominated by the differences in the tag applied to distal spins. FAIR-EPISTAR (d) is an image of large vessels flowing down into the slice. The average of FAIR and EPISTAR (e) is an image of areas perfused by proximally tagged blood, and is very similar to PICORE as demonstrated in (f).

in that it is not directly related to any relaxation time. The lower limit on *TR* is simply the time required for fresh blood to flow into the tagging region. A *TR* that is longer than this does not improve the SNR of the perfusion measurement, and decreases the SNR per unit time. For PICORE QUIPSS II tagging in an axial slice with $TI_1 = 600$ ms, $TI_2 = 1200$ ms, a 10 cm tag, and a 1 cm gap between the tag and the imaging slice, we have determined empirically that there is no significant difference in the ASL signal between *TR*s of 2 and 3 s, indicating that for a *TR* of 2 s, in the 1400 ms between the QUIPSS II saturation pulse and the next inversion tag, fresh blood has flowed into the tag region. For FAIR experiments, the actual length of the tag depends on the B_1 profile of the RF coil used for applying the tag, and longer *TR* may be required. In this study, the RF coil used is relatively short (16 cm total length), and for a typical axial slice through the motor cortex, the FAIR tag is also approximately 10 cm in length. However, in a larger RF coil, the tag in FAIR may be long enough to require the use of a longer TR to allow for inflow of relaxed blood into the tag region.

Data processing

The time series of images that is acquired during a functional ASL experiment is alternated between tag and control states. The simplest method to extract flow information from this time series is pairwise subtraction of images, generating a time series of images that are proportional to flow. However, for any time series that contains BOLD weighting, the signal is modulated not only by perfusion, but also by BOLD contrast. Thus during transitions between off and on states, the overall signal is rising or falling, and images subtracted pairwise would contain signals that are unrelated to perfusion. In order to minimize this effect, we subtract from each image the average of the previous image and the next image, giving a difference signal that is insensitive to linear trends in the overall signal. Higher order signal variations that arise from BOLD contrast or motion will appear in this difference signal, but are typically small. For simultaneous flow and BOLD imaging the flow data is extracted as above, and the BOLD signal is obtained by adding to each image the average of the previous and next images, giving signal that is also insensitive to both flow and local linear trends in the data.

Because the lower limit on *TR* is determined by flow rates to be about 2 s, the intrinsic time resolution of flow measurement techniques is not very high. In some of the studies shown below, the intent is to simultaneously study the dynamics of flow and BOLD contrast. For these studies, we effectively increase the temporal resolution by choosing *TR* such that the stimulus duration differs from an integer multiple of *TR* by *TR*/2. On successive cycles of the functional task, the image acquisition times will be shifted by *TR*/2. In this manner, if the functional response is identical in each task cycle, then images averaged across cycles will have an effective time resolution of *TR*/2, rather than *TR*. In addition, in comparing the time courses of the flow and BOLD signals, we shift the flow signal backwards in time relative to the BOLD signal acquired at the same time. This is because the BOLD signal reflects the state of blood oxygenation and blood volume at the instant of image acquisition, while the flow signal reflects the average flow during the period between the application of the tag and image acquisition. For QUIPSS II, the signal is proportional to the amount of tagged blood that leaves the tagging region in the time TI_1 after the application of the tag. For typical QUIPSS II scan parameters, this time period is 600–1200 ms prior to image acquisition. Taking the average of this time window, we shift the flow data backwards in time by 900 ms in order to properly align the flow data with the BOLD data.

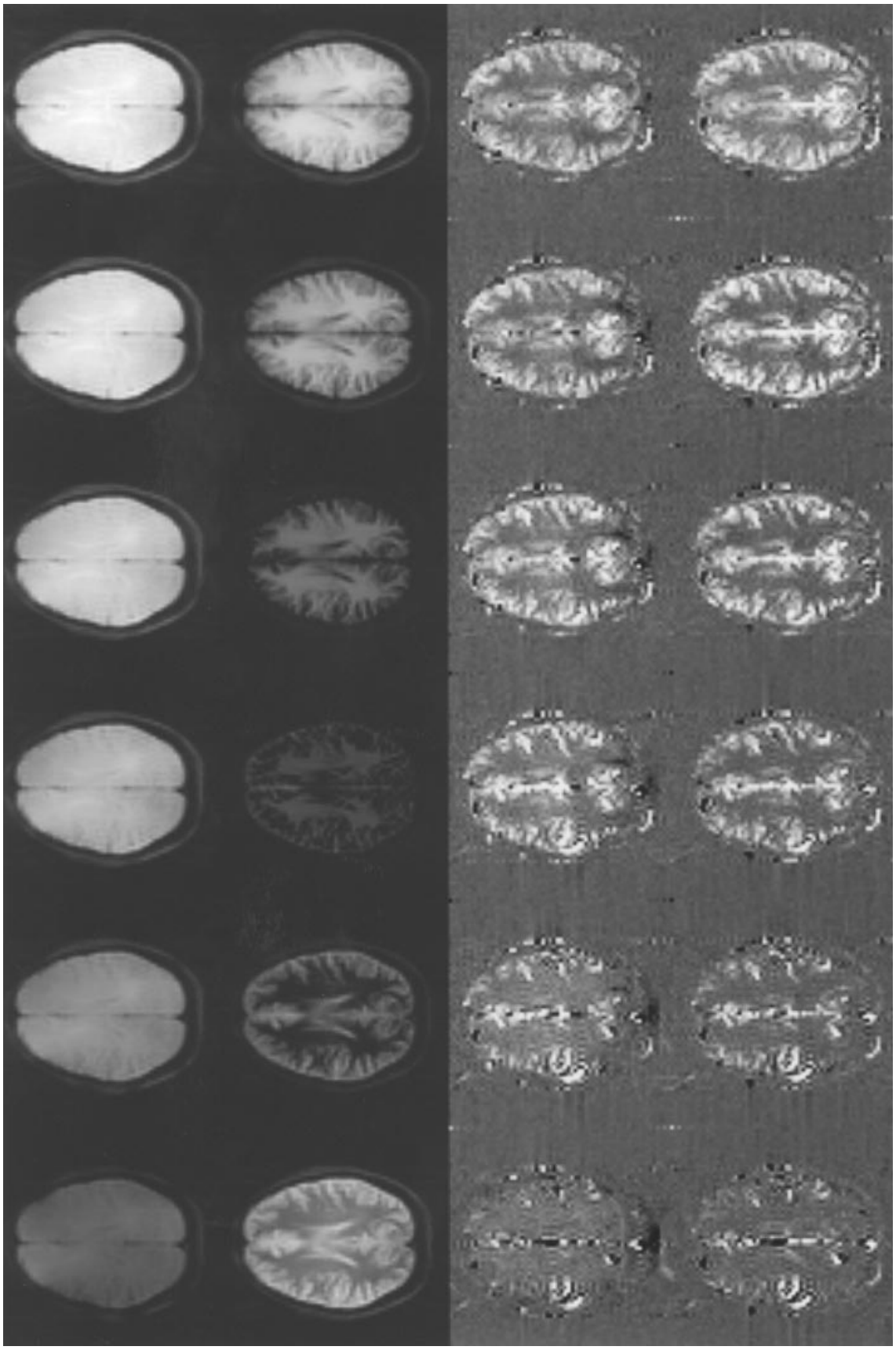

Figure 5. Raw images and difference images (control–tag) for EPISTAR and FAIR as a function of *TI*. From top to bottom: EPISTAR raw images; FAIR raw images; EPISTAR difference images; FAIR difference images. *TI* values from left to right: 200, 400, 600, 800, 1000 and 1200 ms. In this example, FAIR is implemented without in-plane presaturation. While the static tissue contrast is very different, the difference images are dependent only on the inflow of tagged blood.

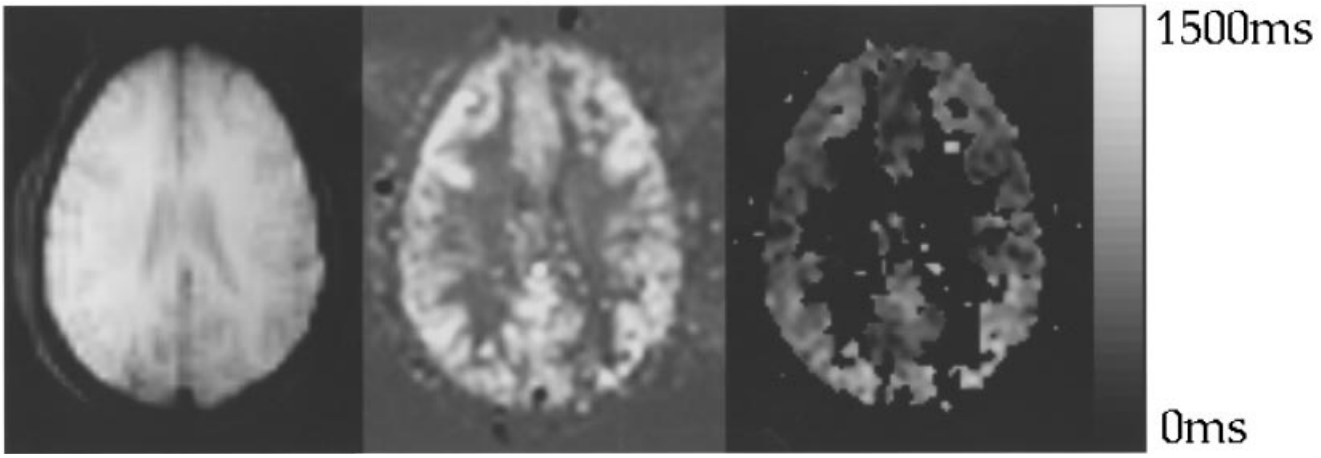

Figure 6. Calculated perfusion and transit delay maps from FAIR images acquired at five values of *TI* (600/850/1100/1350/1600 ms). Perfusion and δt are calculated from the data by numerical fit to Eq. (1). From left to right: anatomical reference; perfusion map; δt map. Transit delay data are only shown for those pixels with high perfusion SNR (gray matter). Other pixels are shown black.

RESULTS

Arterial tagging methods

A comparison of baseline perfusion images using the three tagging techniques is shown in Fig. 4. These images were acquired without the QUIPSS II modification, and are not flow weighted. As expected, contrast in these images is very similar except for focal positive or negative signals that presumably represent larger vessels. Several of these focal signals are positive in the FAIR image, negative in the EPISTAR image, and absent in the PICORE image, consistent with blood flowing into the slice from the distal side. The difference image between EPISTAR and FAIR is dominated by these focal signals, and the average image of EPISTAR and FAIR is nearly identical to the PICORE image.

Figure 5 demonstrates that the difference signal between tag and control states is entirely independent of the tissue contrast in the raw images. For a series of *TI* values, raw unsubstracted images are shown for FAIR without in-plane presaturation and EPISTAR with presaturation. The image contrast is strikingly different, as one is an inversion recovery and the other a saturation recovery. However, in the difference images (control–tag), the perfusion contrast is nearly identical, except for some of the vascular signal as demonstrated above.

Perfusion Quantitation

Figure 6 shows calculated maps of resting perfusion and transit delay δt for a FAIR experiment at *TI* values of 600, 850, 1100, 1350 and 1600 ms, with 6 min of averaging at each value of *TI*. Data were fitted to eq. (1) for parameters f and δt, using an assumed value for T_{1B} (1300 ms), and neglecting q. A small amount of flow weighting (VENC = 1.51 cm/s, $b = 0.94$ s/mm^2) was applied so that the measured delay would reflect the time for the tag to reach brain parenchyma. A typical finding that is illustrated in these data is a very long transit delay in the occipital lobe for axial slices. Measured delays at the occipital pole are typically 1000–1300 ms, as compared to 500–800 ms in the parietal lobes. This is presumably due to differences in the geometry of arteries supplying these regions, with posterior cerebral arteries traveling a long distance parallel to (possibly within) the imaging slice to reach the occipital lobe, while the middle cerebral arteries travel directly superior to the parietal lobes. However, with these differences in delay accounted for, the calculated flow map is relatively uniform. In the individual difference images, the signal in the occipital lobe is significantly lower than in the rest of the cortex at every value of *TI*.

Simultaneous Perfusion and BOLD Imaging

The raw signal timecourse for a group of pixels in a typical combined flow and BOLD finger tapping experiment is shown in Fig. 7. The graphs in the Fig. 7(b) are raw timecourses from the 3×3 matrix of pixels outlined in the image. The rapid oscillation of signal from time point to time point is the flow signal, while the overall rise and fall of the locally averaged signal is the BOLD signal. Also shown in the figure are the timecourses of the separated flow and BOLD signals from the same data. Note that there are several pixels that exhibit a strong BOLD signal, but little or no flow signal.

In an effort to further evaluate the relationship between flow and BOLD, we performed a study in which five subjects were imaged using PICORE/QUIPSS II during a finger tapping task. Representative data from a single subject are shown. The timing of the task was 60 s of tapping followed by 120 s of rest, repeated eight times for a total imaging time of 24 min. The long rest period was used so that the post undershoot of the BOLD signal[18] could be evaluated without contamination from the previous cycle. To improve the effective temporal resolution, a *TR* of 2.01117 was used so that 89.5 images were acquired per functional cycle (3 min). After eight cycles, four cycles had identical timing of the images relative to the task, while the other four were interleaved with the first four, giving an effective time resolution of 1.00559 s. Separate time courses for the flow and BOLD signals were constructed as described above, and each was averaged across the eight functional cycles. Figure 8 shows plots of the averaged single cycle flow and BOLD signals for a 5×5 block of pixels located in the left (in the image) motor area. The time axis of each plot runs from 0–180 s, and the subject was tapping his fingers from time 30 s to 90 s. Large BOLD

changes follow the central sulcus. The flow time courses are noisier, but show changes that are roughly parallel to the BOLD changes. However, there are some interesting variations. A few pixels in the lower right corner exhibit BOLD changes without evident flow changes, and several of the pixels with prominent BOLD changes also show a post-stimulus undershoot. For each time course the absolute signal change was calculated by averaging the time points during the stimulus and subtracting the average of the baseline. Figure 9 shows maps of flow and BOLD signal change along with an anatomical image. Note that regions with a large BOLD change do not necessarily correspond to regions of large flow change. In order to characterize this effect further, two blocks of 8×8 pixels were chosen from each motor area for further analysis. Pixels with a BOLD signal change greater than 0.5% were identified (34 pixels) and were then divided into two groups based on flow change: a large flow group that had a flow signal change that was greater than 0.4% of the raw image signal (19 pixels); and a small flow group that had a flow signal change that was less than 0.4% (15 pixels). The averaged time courses for these two groups are shown in Fig. 10. In these plots, the flow signal has been normalized to the average signal value in the raw images in order to facilitate comparison of the flow and BOLD signal changes. Thus, a flow change of 0.4% is measured relative to the raw signal; the fractional change in the flow signal itself with activation is much larger (typically about 50%). The plateau value of the BOLD signal change is comparable in the two groups, but the large flow group shows a pronounced post-stimulus

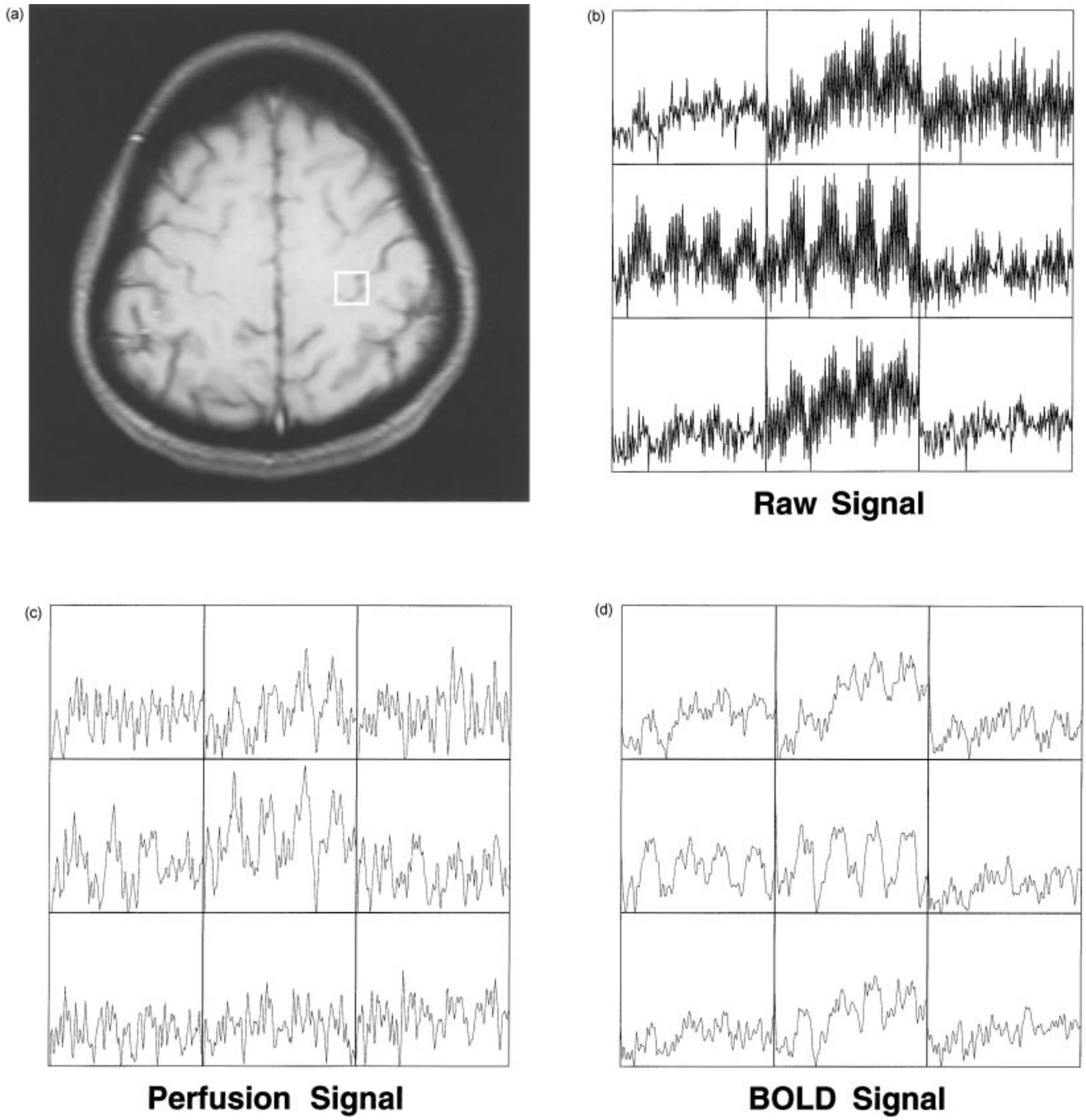

Figure 7. Separation of raw signal from a simultaneous flow and BOLD experiment into flow and BOLD components. (a) Anatomical image showing the region from which graphs are taken. (b) Raw time signal from the 3×3 matrix of pixels outlined in (a). The graph in each box is the time domain signal from one pixel through four periods of finger tapping interleaved with five periods of rest. (c) Flow signal. (d) BOLD signal. See text.

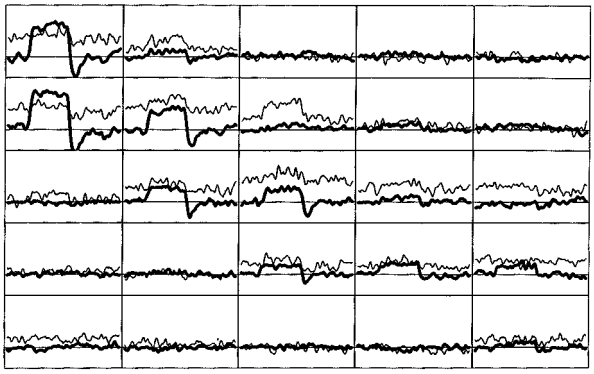

Figure 8. Flow (fine lines) and BOLD (heavy lines) signal for a 5×5 block of pixels in the motor area during a finger tapping test. The time signal from eight periods of finger tapping were separated into flow and BOLD components and averaged (see text). Note prominent post-stimulus undershoot in the BOLD signal in some pixels, but no undershoot in the flow signal.

undershoot in the BOLD signal. The corresponding flow signal, and the BOLD signal from the low flow group, do not show an undershoot. Data from identical experiments on four other subjects demonstrate this same phenomenon. The origin of the post stimulus undershoot is controversial, but we have postulated that it is caused by a slow decrease in blood volume relative to the decrease in flow after cessation of the stimulus. We have recently proposed a simple biomechanical model for the relationship between flow, blood volume, and BOLD signal that is consistent with these data and suggest that the undershoot may be a function of the capacitance of small veins in the presence of continuous and tight coupling between flow and O_2 metabolism.[2]

Multislice ASL

Examples of a multislice baseline perfusion data set acquired using PICORE and QUIPSS II are shown in Fig. 11. This data set was acquired using 144 averages and a *TR* of 2 s, for a total imaging time of 4 min 48 s. Note that subject to the assumptions of the validity of eqs. (4–5) and

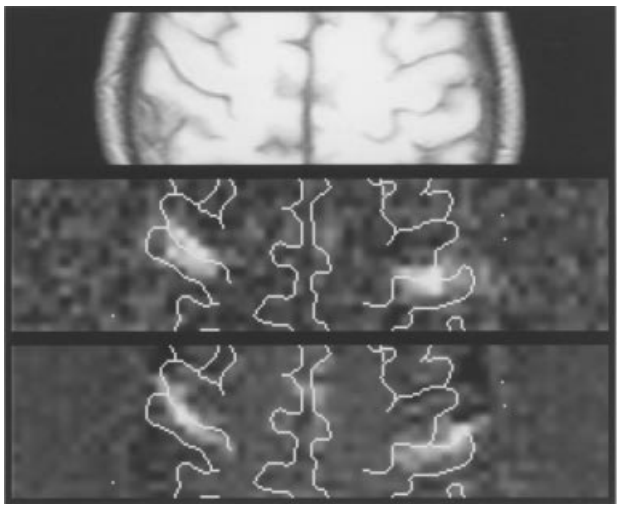

Figure 9. Flow change and BOLD change maps from the same experiment as in Fig. 8. From top: anatomical reference; flow signal change map; BOLD signal change map. The largest BOLD changes are restricted to the sulcus, while the flow change has a wider distribution, is centered more medially, and appears on the left to lie in two lines straddling the sulcus.

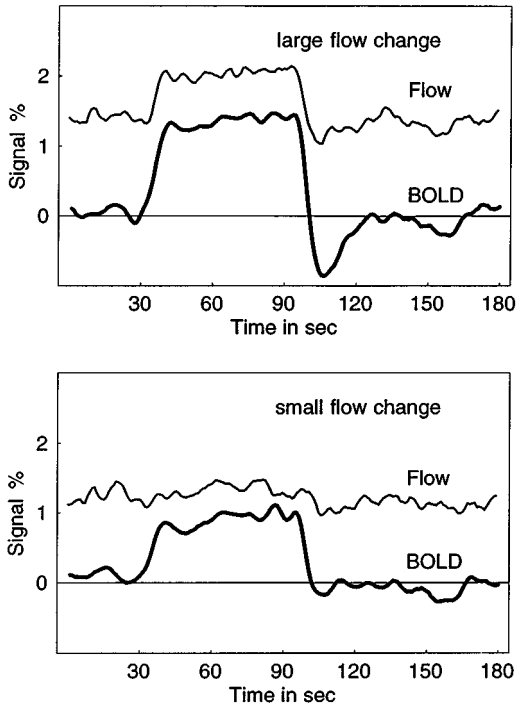

Figure 10. Averaged time courses for functionally activated pixels. Pixels demonstrating a BOLD change were divided into a large flow group (top, 19 pixels) and a small flow group (bottom, 15 pixels). The BOLD signal shows a prominent post-stimulus undershoot in the high flow pixels, but not in the low flow pixels. The flow signal does not show an undershoot.

small residual imperfections of the inversion slice profiles, these perfusion maps are quantitative, and approach the quality of the perfusion map of Fig. 6, which is calculated from 30 min of scanning. For comparison, a perfusion image of the middle slice, acquired a single slice data is also shown. The flow images appear qualitatively correct, but there is a small systematic error in the images across slices that is approximately 0.25% of the raw signal at the first and last slices due to slice profile effects. The flow signal itself is approximately 1% of the raw signal in gray matter. While this error affects quantitation of the absolute perfusion, it does not affect the measured amplitude of the functional perfusion change because it is a constant offset in the perfusion signal. During this same experiment the subject performed two periods of finger tapping, and maps of the functional change in the perfusion and BOLD signals are shown in Fig. 12. In this figure, the results of a correlation analysis are displayed rather than the functional change itself, as in Fig. 9. Pixels drawn white have a correlation coefficient with a reference function of $r > 0.4$, while those drawn black have $r < -0.4$.

SUMMARY

In the implementation of pulsed ASL perfusion imaging techniques for fMRI, there are several sources of error that can significantly affect the dynamic perfusion measurement. The most important of these are the transit delay and the presence of intravascular tagged signal, both of which not only vary across a slice, but also vary through time in the presence of functional activation. QUIPSS II is a modification of the basic pulsed ASL technique that can be made insensitive to these sources of error in a dynamic measure-

ment. For applications in pathological conditions such as stroke or the presence of brain tumors it is particularly important to use techniques that are insensitive to large variations in transit delay. In these applications, cerebral

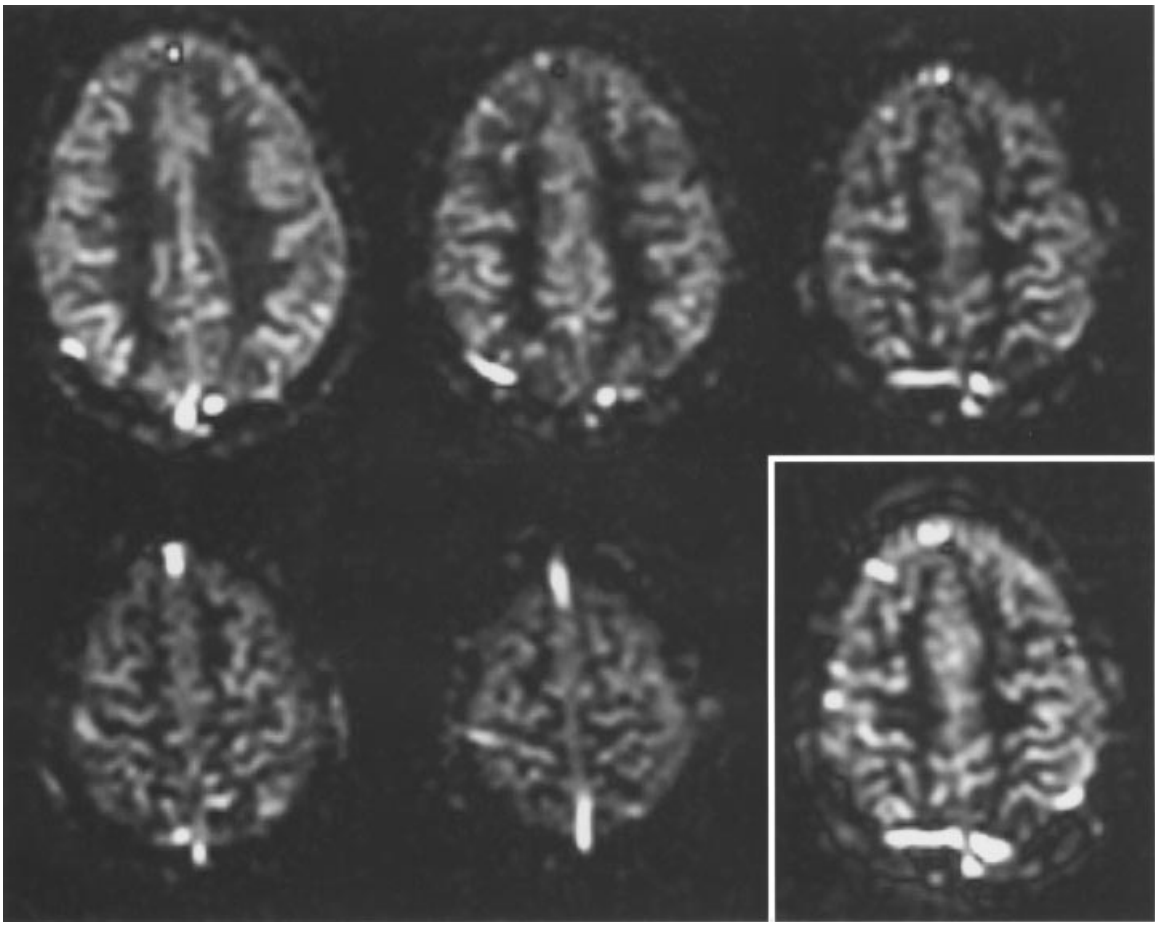

Figure 11. Multislice baseline perfusion maps. Five 6 mm contiguous slices were acquired in 4 min 48 s of averaging using PICORE QUIPSS II. The three images in the top row and the first two in the second row are the five slice set. Images were acquired from inferior to superior 80 ms apart, and the more distal slices were corrected in overall amplitude for increased T_1 decay relative to the proximal slice. The lower right image is a single slice perfusion measurement of the center slice of the multislice set (upper right slice), acquired in the same imaging time.

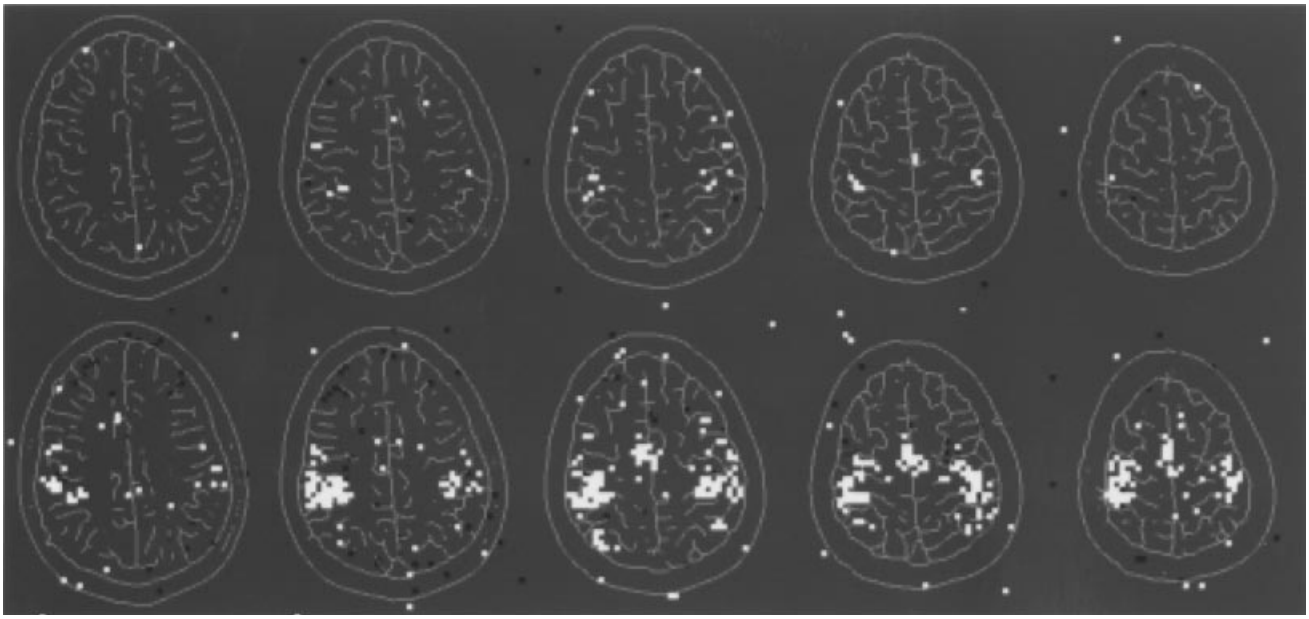

Figure 12. Functional maps generated from the five slice data set shown in Fig. 11. Data were separated into flow and BOLD components and all pixels with $r > 0.4$ are shown in white, while those with $r < -0.4$ are shown in black. Top row is flow, bottom row is BOLD.

vasculature is likely to be abnormal, and transit delays may be very long. While QUIPSS II can in principle be made insensitive to any transit delay, some *a priori* information about the range of transit delays is necessary in order to optimally select imaging parameters.

Multislice pulsed ASL is feasible for moderate numbers of slices (≈ 5). Imperfect subtraction of static tissue signal appears to be fundamentally different in pulsed ASL than in continuous ASL, as is consistent with slice profile effects in the former, and MT effects in the latter. Careful selection of parameters for sech inversion pulses can dramatically improve the quality of the static tissue subtraction in pulsed ASL, and we expect that further improvements are forthcoming.

In the collection of simultaneous flow and BOLD data, it is important to control the static tissue contrast so that flow and BOLD information can be clearly separated. While the BOLD effect derives from changes in flow, flow and R_2* (or R_2) changes can be separated with minimal contamination. This is supported experimentally by the fact that both the maps and the timecourses of changes in these two quantities during activation are distinctly different.

We believe that the timecourse and distribution of flow and BOLD changes is supportive of the idea that BOLD changes occur both in brain parenchyma and in large veins, and the perfusion signal is more well localized to brain parenchyma. However, the greater spatial specificity of functional flow imaging is offset by lower sensitivity. This suggests a strategy whereby BOLD imaging is used to find approximate areas of activation for a specific task, and incorporated as *a priori* information in the search for areas with significant flow changes.

For the study of functional MRI contrast mechanisms, it is particularly valuable that flow and BOLD information can be collected simultaneously because the dynamics of the BOLD signal change depend on the dynamics of the flow change. We are hopeful that this information, along with information about local blood volume, will provide the basis for quantitative interpretation of the BOLD signal change.

REFERENCES

1. Bandettini, P. A., Wong, E. C., Hinks, R. S., Tikofsky, R. S. and Hyde, J. S. Time course EPI of human brain function during task activation. *Magn. Reson. Med.* **25**, 390–397 (1992).
2. Buxton, R. B. and Frank, L. R. A model for the coupling between cerebral blood flow and oxygen metabolism during neural stimulation. *J. Cereb. Blood Flow Metab.* **17**, 64–72 (1997).
3. Edelman, R. R., Siewert, B., Adamis, M., Gaa, J., Laub, G. and Wielopolski, P. Signal targeting with alternating radio frequency. *Magn. Reson. Med.* **31**, 233–238 (1994).
4. Kwong, K. K., Chesler, D. A., Weisskoff, R. M. and Rosen, B. R. Perfusion MR imaging. In *Proc., SMR*, 2nd Meeting, San Francisco, 1994, p. 1005.
5. Buxton, R. B., Wong, E. C. and Frank, L. R. Quantitation issues in perfusion measurement with dynamic arterial spin labeling. In *ISMRM*, 4th Meeting, New York, 1996, p. 10.
6. Buxton, R. B., Frank, L. R., Siewert, B., Warach, S. and Edelman, R. R. A quantitative model for EPISTAR perfusion imaging. In *SMR*, Third Meeting, Nice, France, 1995, p. 132.
7. Ye, F. Q., Pekar, J. J., Jezzard, P., Duyn, J., Frank, J. A. and McLaughlin, A. C. Perfusion imaging of the human brain at 1.5 T using a single shot EPI spin tagging approach. *Magn. Reson. Med.* **36**, 217–224 (1996).
8. Wong, E. C., Frank, L. R. and Buxton, R. B. QUIPSS II: a method for improving quantitation of perfusion using pulsed arterial spin labeling. In *ISMRM*, 5th Meeting, Vancouver, (1997), p. 1761.
9. Wong, E. C., Buxton, R. B. and Frank, L. R. Quantitative imaging of perfusion using a single subtraction (QUIPSS). *Neuroimage* **3**, S5 (1996).
10. Wong, E. C., Buxton, R. B. and Frank, L. R. The effects of diffusion weighting in pulsed arterial spin labeling. *Magn. Reson. Med.* (submitted).
11. Alsop, D. C. and Detre, J. A. Reduced transit time sensitivity in noninvasive magnetic resonance imaging of human cerebral blood flow. *J. Cereb. Blood Flow Metab.* **16**, 1236–1249 (1996).
12. Boxerman, J. L., Bandettini, P. A., Kwong, K. K., Baker, J. R., Davis, T. L., Rosen, B. R. and Weisskoff, R. M. The intravascular contribution to fMRI signal change: Monte Carlo modeling and diffusion-weighted studies *in vivo*. *Magn. Reson. Med.* **34**, 4–10 (1995).
13. Pekar, J., Jezzard, P., Roberts, D. A., Leigh, J. S., Frank, J. A. and McLaughlin, A. C. Perfusion imaging with compensation for asymmetric magnetization transfer effects. *Magn. Reson. Med.* **35**, 70–79 (1996).
14. Silver, M. S., Joseph, R. I. and Hoult, D. I. Selective spin inversion in nuclear magnetic resonance and coherent optics through an exact solution of the Bloch-Riccati equation. *Phys Rev. A* **31**, 2753–2755 (1985).
15. Frank, L. R., Wong, E. C. and Buxton, R. B. Slice profile effects in adiabatic inversion: application to multi-slice perfusion imaging using pulsed arterial spin labelling. In *ISMRM,* 5th Meeting, Vancouver (1997), p. 1755.
16. Wong, E. C., Bandettini, P. A. and Hyde, J. S. Echo-planar imaging of the human brain using a three axis local gradient coil. In *Proc., SMRM,* 11th Annual Meeting, Berlin, 1992, p. 105.
17. Wong, E. C., Boskamp, E. and Hyde, J. S. A volume optimized quadrature elliptical endcap birdcage brain coil. In *Proc., SMRM*, 11th Annual Meeting, Berlin, 1992, p. 4015.
18. Davis, T. L., Weisskoff, R. M., Kwong, K. K., Savoy, R. and Rosen, B. R. Susceptibility contrast undershoot is not matched by inflow contrast undershoot. In *SMR*, 2nd Annual Meeting, San Francisco, 1994, p. 435.